The $K_{\pi 2}$ scatter 1/3 background

Ilektra A. Christidi, Stony Brook

June 21, 2007

Abstract

This note describes the measurement of the target and RS $K_{\pi 2}$ background with the 1/3 skimmed data on disk, processed in May '07. A small part of the data is missing from this sample, thus the measurement has to be redone after the reprocessing of the data on tape.

1 $K^+ \to \pi^+ \pi^o$ Target (TG) scatters

The $K_{\pi 2}$ decay, where the π^+ scatters in the Target, is the dominant background for the $\pi\nu\overline{\nu}(2)$ analysis. As it has been shown with Monte Carlo simulations [1], the photon distribution from the π^o decay is more uniform in polar angle for events where the π^+ has scattered in the target, than for unscattered ones. Therefore, the PV rejection for TG scatter events is expected to be different than that for $K_{\pi 2}$ events in the peak. The π^+ kinematics cannot be used in the bifurcation study, since the PV rejection has to be measured inside the $\pi\nu\overline{\nu}(2)$ kinematic box.

The other set of cuts used to supress this background are the target quality cuts (TGCUT06). These eliminate events with evidence of a scattered pion in the target, either the scatter occured outside the Kaon fibers (scatters visible in xy, or "xy-scatters") or inside them (events where the π^+ started in the beam direction and then scattered into the detector acceptance, or "z-scatters"). The two categories are not mutually exclusive. By inverting some of these cuts and applying others, samples with varying mixtures of xy- and z-scatters can be created for the rejection branch. These samples will be contaminated to an extent with K_{e4}, $K_{\pi 2\gamma}$ and Charge Exchange background, but the contamination is shown to be small (see later section). Thirteen such "classes" were used, described in Table 1, and the PV rejection was measured on them in the $\pi\nu\overline{\nu}(2)$ kinematic box (Table 2). The rejection in the $K_{\pi 2}$ peak is also given for comparison. The PV rejections measured for different classes are consistent with each other within statistical uncertainties.

For the final PV rejection, class 12 was used, because it had adequate statistics and it is expected to be the richest in z-scatters, since the cuts that majorly attack them are inverted: CCDPUL and EPIONK cut events with large pulses in the kaon fibers at trs, and B4EKZ rejects events in which the z position of the decay vertex found by the UTC does not agree with the kaon energy deposit (and thus path length) in the target. Both these signatures are characteristic of a decay pion that started in the beam direction in the kaon fiber, and then scattered into the detector. The second pulse energy distribution for class 12, $K_{\pi 2}$ peak events, and $K_{\mu 2}$ events is shown in Fig. 1. The

CLASS	TGCUTS
1	All cuts, KP2BOX
2	$\overline{CCDPUL}$, $\overline{EPIONK}$
3	$\overline{CCDPUL}$, $\overline{EPIONK}$, all others
4	CCDPUL, EPIONK, TGZFOOL, EIC, OPSVETO, $\overline{OTHERS}$
5	$\overline{CCDPUL}$, $\overline{EPIONK}$, $\overline{CHI567}$, $\overline{VERRNG}$
6	$\overline{CCDPUL}$, $\overline{EPIONK}$, $\overline{CHI567}$, $\overline{VERRNG}$, all others
7	$\overline{CHI567}$, $\overline{VERRNG}$
8	$\overline{CHI567}$, $\overline{VERRNG}$, all others
9	$\overline{CCDPUL}$, $\overline{EPIONK}$, $\overline{CHI567}$, $\overline{VERRNG}$, KIC, PIGAP, TARGF, TPICS
10	$\overline{B4EKZ}$
11	$\overline{B4EKZ}$, all others
12	$\overline{CCDPUL}$, $\overline{EPIONK}$, $\overline{B4EKZ}$
13	$\overline{CCDPUL}$, $\overline{EPIONK}$, $\overline{B4EKZ}$, all others

Table 1: Definition of the classes of events (2-13) used to measure the PV rejection in the $\pi\nu\overline{\nu}(2)$ kinematic box. Class 1 events have passed all the TG quality cuts, therefore they are required to be in the $K_{\pi 2}$ kinematic box.

difference in PV rejection between different classes with adequate statistics was used as an estimate for the systematic uncertainty.

In the normalization branch (see Table 3), all the cuts in TGCUT06 were applied, and the PV was inverted. Some contamination from $K_{\pi 2}$ RS scatters and $K_{\pi 2\gamma}$ is expected, but these backgrounds are small compared to $K_{\pi 2}$ TG scatters. The ptot distribution of the events remaining in the normalization branch after the inversion of PVCUTPNN2, after the application of all the TGCUT06 except CCDPUL, and after the application of CCDPUL is shown in Fig. 2. In the same figure, the ptot distribution of the events in class 12 of the rejection branch is also shown before and after PVCUTPNN2. Both of those distributions look adequately $K_{\pi 2}$-scatter-like.

Using the numbers from tables 3 and 2, the $K_{\pi 2}$ target scatter background is

$$N_{K_{\pi 2}-TGscat} = 3 \times \frac{N}{R_{PVclass12} - 1} = 3 \times \frac{498}{(2540.4 \pm 765.8) - 1} = 0.588 \pm 0.178(stat.)^{+0.067}_{-0.222}(sys.) \quad (1)$$

The systematic error comes from the difference in background predicted by the class with the highest (CLASS7) and lowest (CLASS9) PV rejection, with respect to the central value from CLASS12. Only classes with adequate statistics are considered.

1.1 PV rejection profiles

Due to the lack of statistics in the 12 rejection classes of $K_{\pi 2}$ TG-scattered events defined in Table 1, the PV parameters were optimized in the $K_{\pi 2}$ peak. The result in the $K_{\pi 2}$ peak, broken down to each subsystem contribution, is shown in Fig. 3. Then the same PV was applied to the 12 TG-scatter classes, and the profiles of Fig. 4-Fig. 9 were obtained (only the most populous classes are shown). The values at 60% acceptance were chosen for the nominal/loose box, and the ones at 30% for the

CLASS	PNN2BOX				KP2BOX		
	bef. PV	af. PV	rejection	bg (3/3)	bef. PV	af. PV	rejection
1					56196	35	1605.6±271.3
2	25828	10	2582.8±816.6	0.579±0.183	155269	134	1158.7±100.1
3	2547	3	849.0±489.9	1.762±1.018	56918	55	1034.9±139.5
4	4469	3	1489.7±859.8	1.004±0.580	67715	48	1410.7±203.5
5	31681	13	2437.0±675.8	0.613±0.170	193431	163	1186.7±92.9
6	3661	3	1220.3±704.3	1.225±0.708	79626	72	1105.9±130.3
7	24498	6	4083.0±1666.7	0.366±0.150	92462	65	1422.5±176.4
8	267	1	-	-	11173	9	1241.4±413.6
9	25085	11	2280.4±687.4	0.655±0.198	181864	157	1158.4±92.4
10	10840	4	2710.0±1354.8	0.551±0.276	29393	28	1049.8±198.3
11	50	1	-	-	2853	3	951.0±548.8
12	27944	11	2540.4±765.8	0.588±0.178	167727	143	1172.9±98.0
13	3051	3	1017.0±586.9	1.470±0.850	62835	59	1065.0±138.6

Table 2: The rejection branch for the $K_{\pi 2}$ TG scatter background: PV rejection for the $\pi\nu\overline{\nu}(2)$ and $K_{\pi 2}$ boxes, and respective background, for the 12 classes. The classes that are skipped do not have enough statistics for a meaningful measurement. The same setup cuts as in the normalization branch (Table 3) are applied.

tight box. These parameters can be found in [2], and more details about the optimization and the AD in [3],[4].

1.2 Rejection sample purity

The 14 events surviving after all cuts in the rejection branch in all classes (there is significant overlap between the classes) were examined, in order to identify any contamination with K_{e4} or other backgrounds, which would give a wrong PV rejection measurement. The results of this inspection are shown in Table 4. It can be seen that class 12, which is used for the PV rejection measurement, mostly consists of $K_{\pi 2}$ scatters. Event displays of the K_{e4} the possible K_{e4} and the 2-beam event of class 12 are shown in Fig. 10-Fig. 12. More details in [5].

2 $K^+ \to \pi^+\pi^o$ Range Stack scatters

Pions from the $K_{\pi 2}$ decay can also undergo inelastic scattering in the Range Stack and fall into the $\pi\nu\overline{\nu}(2)$ kinematic box by losing energy in the scattering process. However, for these events to be a background for this analysis, the pion momentum also has to be mis-measured and the photons from the π^o decay have to be missed. Therefore, this background is expected to be smaller compared to the $K_{\pi 2}$ target scattered background.

It should be noted that these background events are already included in the normalization branch in Table 3[1], but they are not included in the rejection branch in Table 2 because the target cuts were

[1] Correcting the normalization of $K_{\pi 2}$ TG scatters for $K_{\pi 2}$ RS scatters does not make a significant difference in the

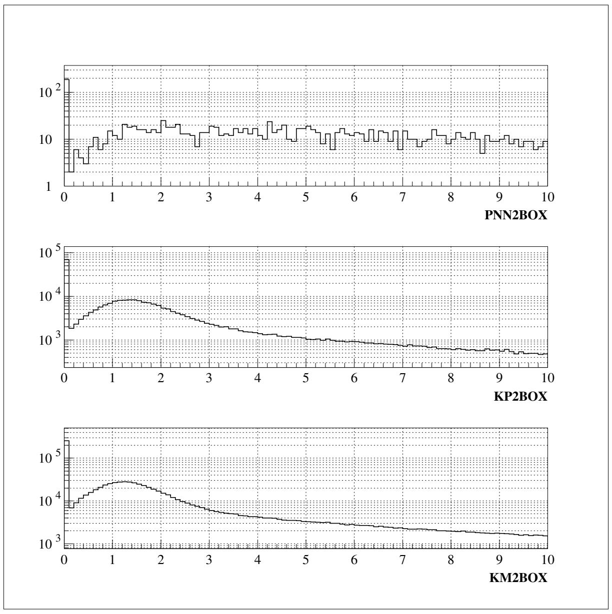

Figure 1: Energy distribution of the second pulse in the Kaon fiber for class 12 of the $K_{\pi 2}$ TG scatter rejection branch (top), for $K_{\pi 2}$ peak events (middle) and for $K_{\mu 2}$ events (bottom).

reversed to measure this PV rejection. The $K_{\pi 2}$ events which scattered in the RS should be assigned the same Photon Veto rejection as the $K_{\pi 2}$ peak events, since the pion did not scatter in the target.

The most effective cuts against this background are the Range Stack track quality cuts RSDEDX and PRRF (collectively referred to as RSCT), the BOX cut on *ptot* and the Photon Veto cut. Table 5 summarizes this background study. The SETUP cuts are the same as the $K_{\pi 2}$ target scatter normalization branch. The second and the third columns of the table contain events in the $K_{\pi 2}$ momentum peak. Events with the momentum of the $K_{\pi 2}$ peak events, but lowered in range and energy are assumed to have scattered in the Range Stack.

The efficiency ϵ_{RSCT} and the rejection R_{RRSCT} of these cuts can be measured as

$$\begin{aligned} \epsilon_{RSCT} &= 56196/76030 &= 0.739 \pm 0.002 \\ R_{RSCT} &= 602/78 &= 7.718 \pm 0.815 \end{aligned} \tag{2}$$

The fourth and fifth column of Table 5 are for normalization. The RSCT cut is reversed and all other cuts are applied. The various contributions to the total 154 events left in the PNN2BOX before the application of the PV have to be considered in order to calculate the background of interest. The largest component of this sample comes from scattering in the target that contaminated the RSCT reversed sample because of the inefficiency of the RSCT cuts. On the other hand, the total 498 events in the $K_{\pi 2}$ target scatter normalization branch (Table 3) have a target scattered (N_{tg}) and a RS scattered (N_{rs}) component. Therefore

$$\begin{aligned} N_{tg} + N_{rs} &= 498 \\ (1 - \epsilon_{RSCT}) \times N_{tg} + (R_{RSCT} - 1) \times N_{rs} &= 154 \end{aligned} \tag{3}$$

background, given the statistical uncertainty.

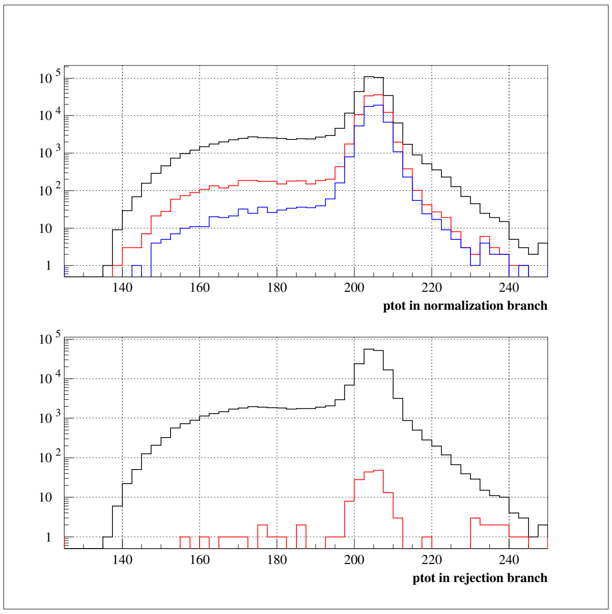

Figure 2: Top: ptot distribution of the events remaining in the normalization branch of the $K_{\pi 2}$ TG scatter study after the inversion of PVCUTPNN2 (black), after the application of all the TGCUT06 except CCDPUL (red), and after the application of CCDPUL (blue). Bottom: ptot distribution of the events in class 12 of the rejection branch of the $K_{\pi 2}$ TG scatter study before (black) and after (red) PVCUTPNN2.

Solving this system of equations, the real $K_{\pi 2}$ RS scatter normalization is obtained, $N_{rs} = 3.730 \pm 0.494$. The final background from the RS scattered events can be measured by applying the $K_{\pi 2}$ peak Photon Veto rejection to N_{rs} from the second column of Table 5, $R_{PV-K_{\pi 2}peak} = 56196/35 = 1605.6 \pm 271.3$:

$$N_{K_{\pi 2}-RSscat} = 3 \times \frac{N_{rs}}{R_{PV-K_{\pi 2}peak} - 1} = 0.007 \pm 0.002 \qquad (4)$$

References

[1] V. Jain, 'Simulation of elastic scatters of π^+ in the target from Kp2 decays', E787 technical note 375, 1999.

[2] `http://www.phy.bnl.gov/e949/software/meetings/bnl/19jun07/pvparams.ps`

[3] I. Christidi, PhD thesis.

[4] I. Christidi, 'The Active Degrader', E949 technical note K-065, 2006.

[5] `http://www.phy.bnl.gov/e949/software/meetings/bnl/kp2scat_rej_events`

[6] `http://www.phy.bnl.gov/~benjil`

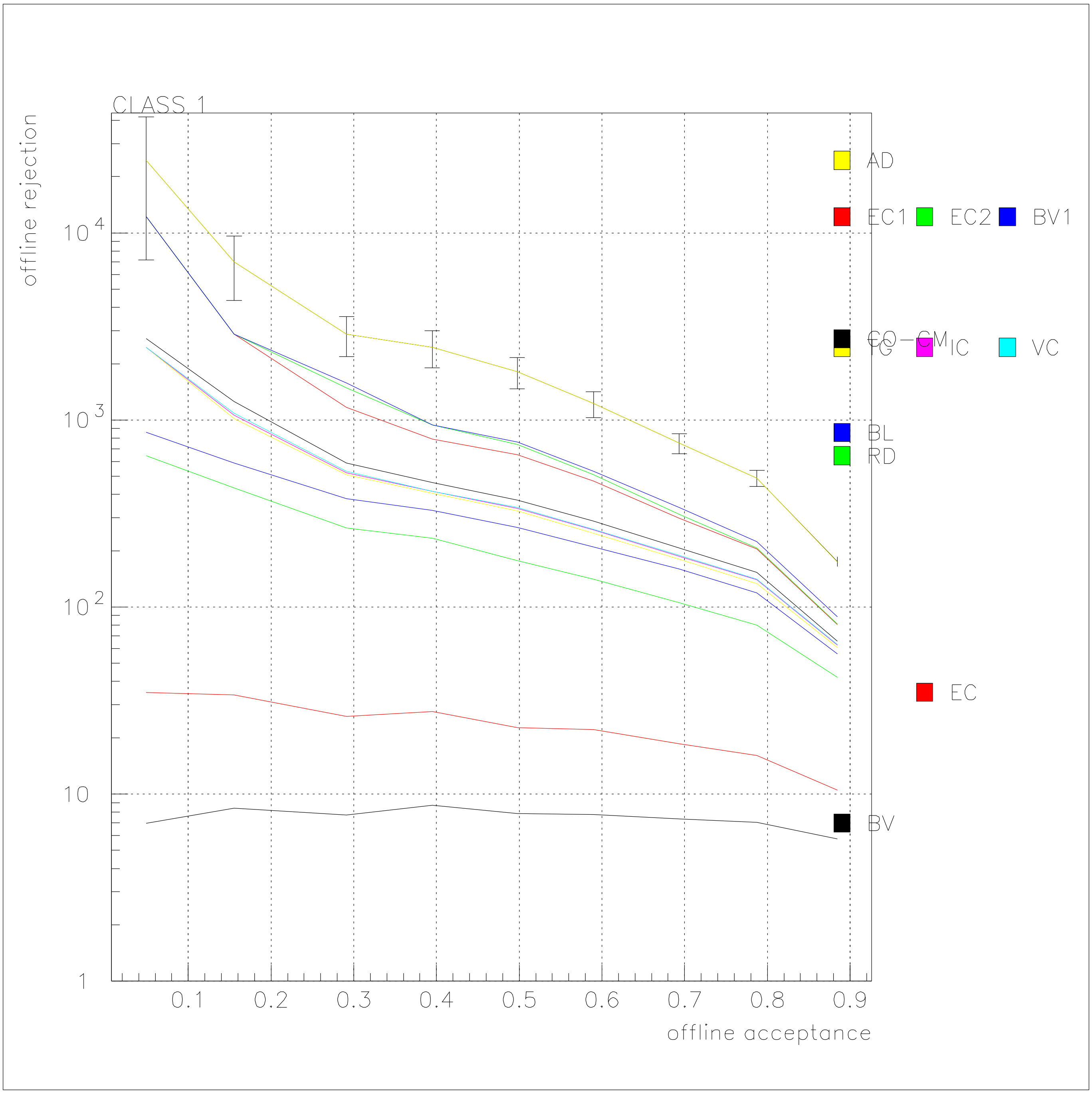

Figure 3: Offline rejection vs acceptance profile for the $K_{\pi 2}$ peak, with each subsystem contribution.

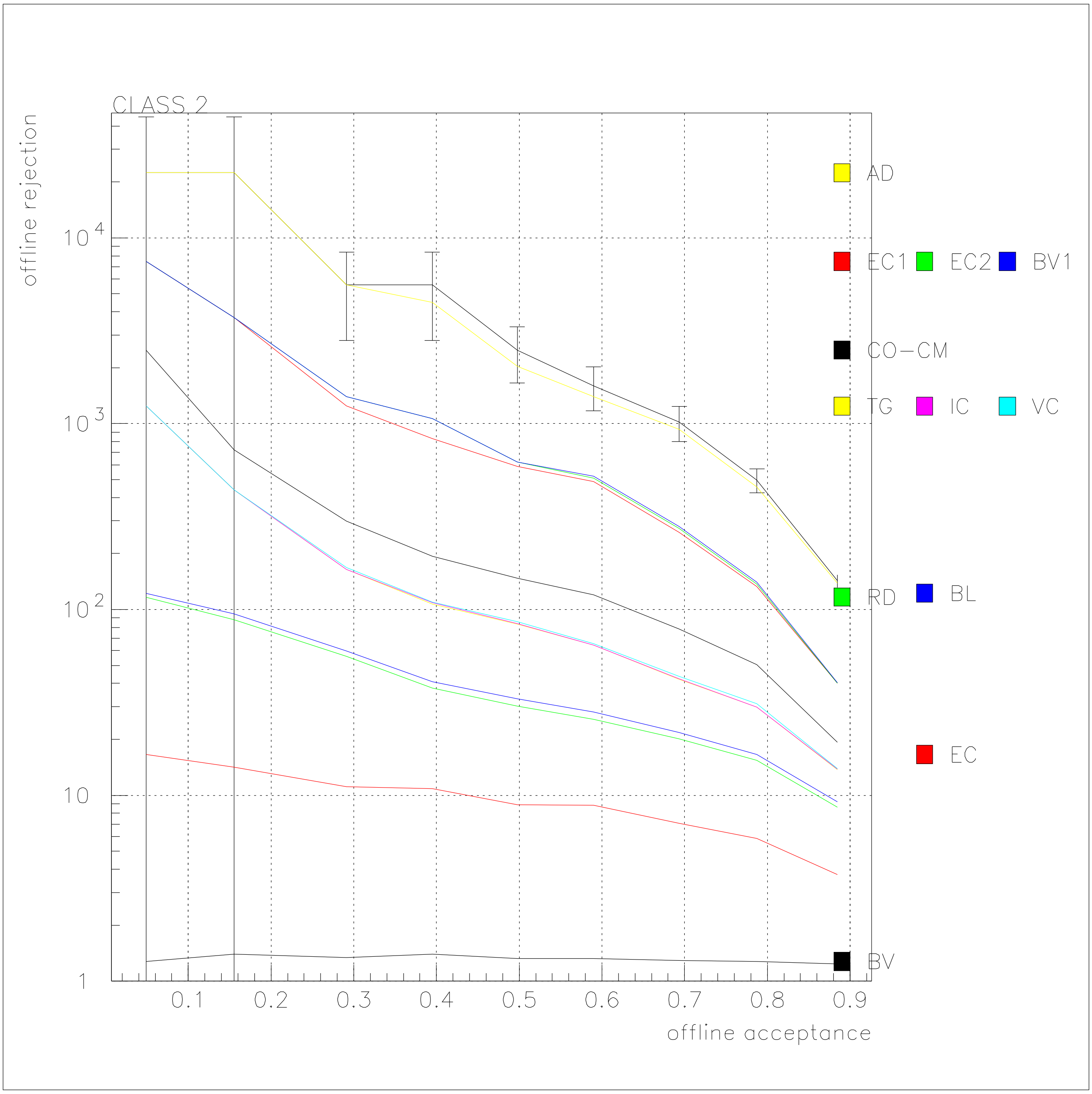

Figure 4: Offline rejection vs acceptance profile for class 2, with each subsystem contribution.

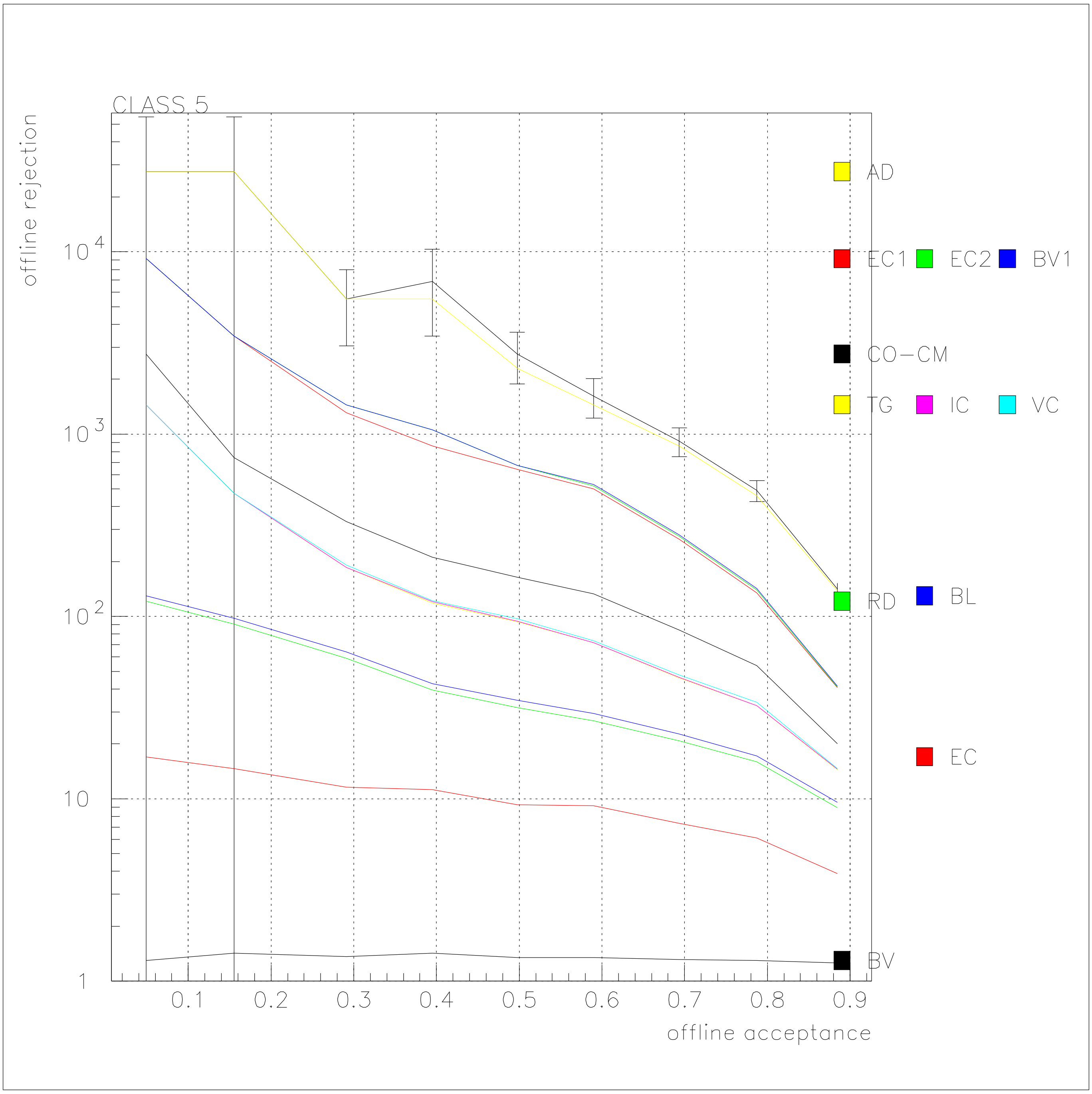

Figure 5: Offline rejection vs acceptance profile for class 5, with each subsystem contribution.

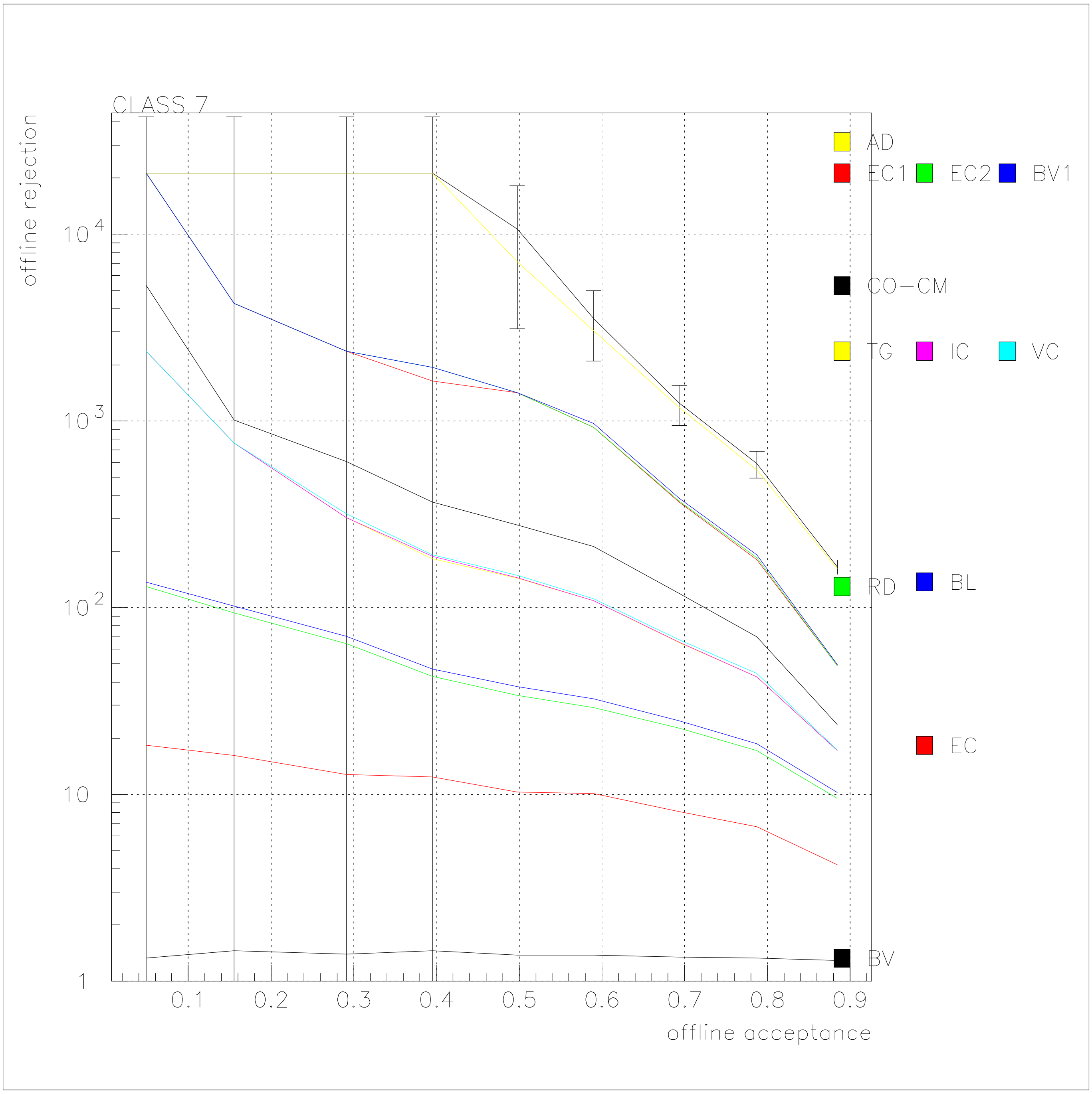

Figure 6: Offline rejection vs acceptance profile for class 7, with each subsystem contribution.

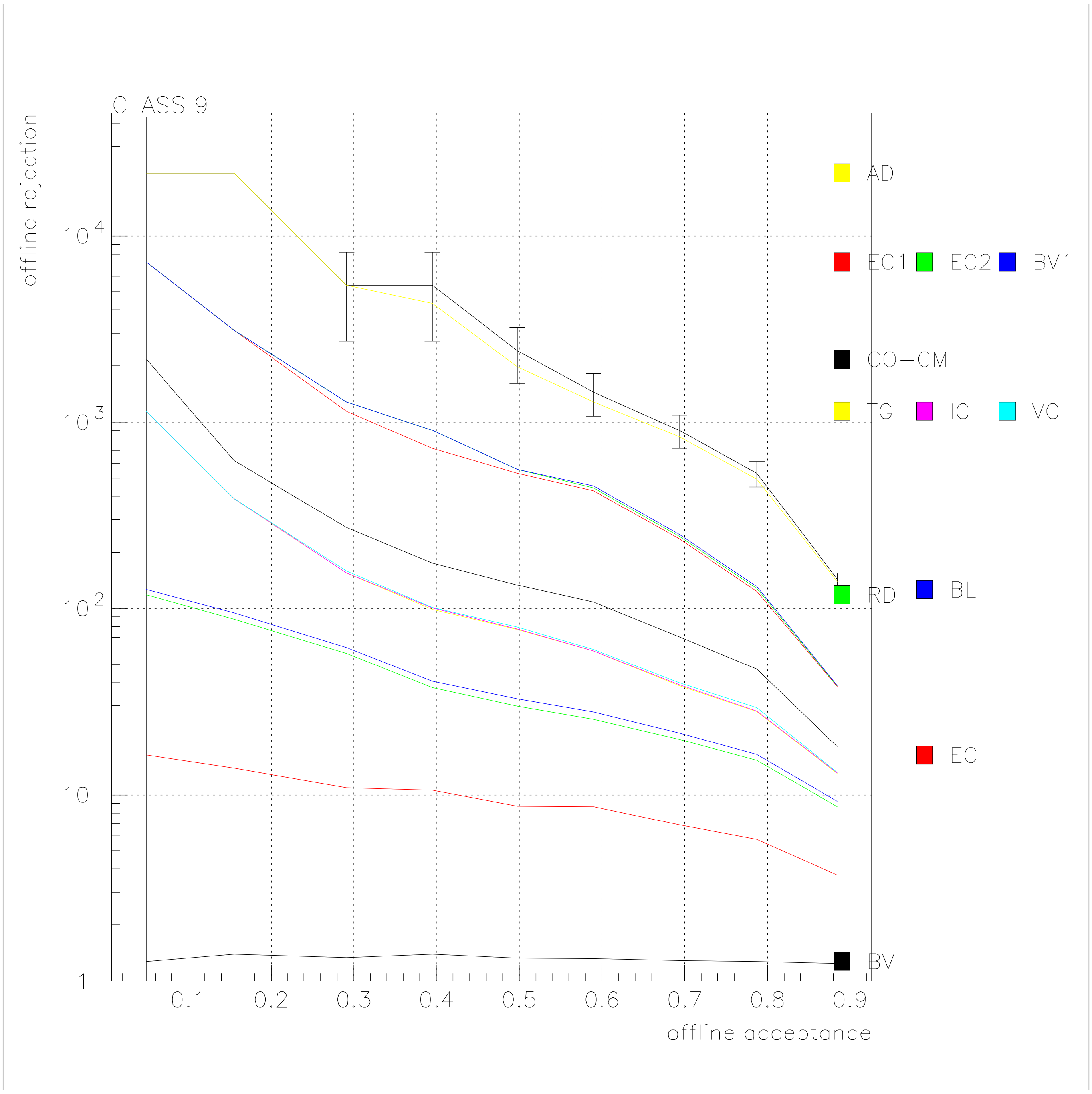

Figure 7: Offline rejection vs acceptance profile for class 9, with each subsystem contribution.

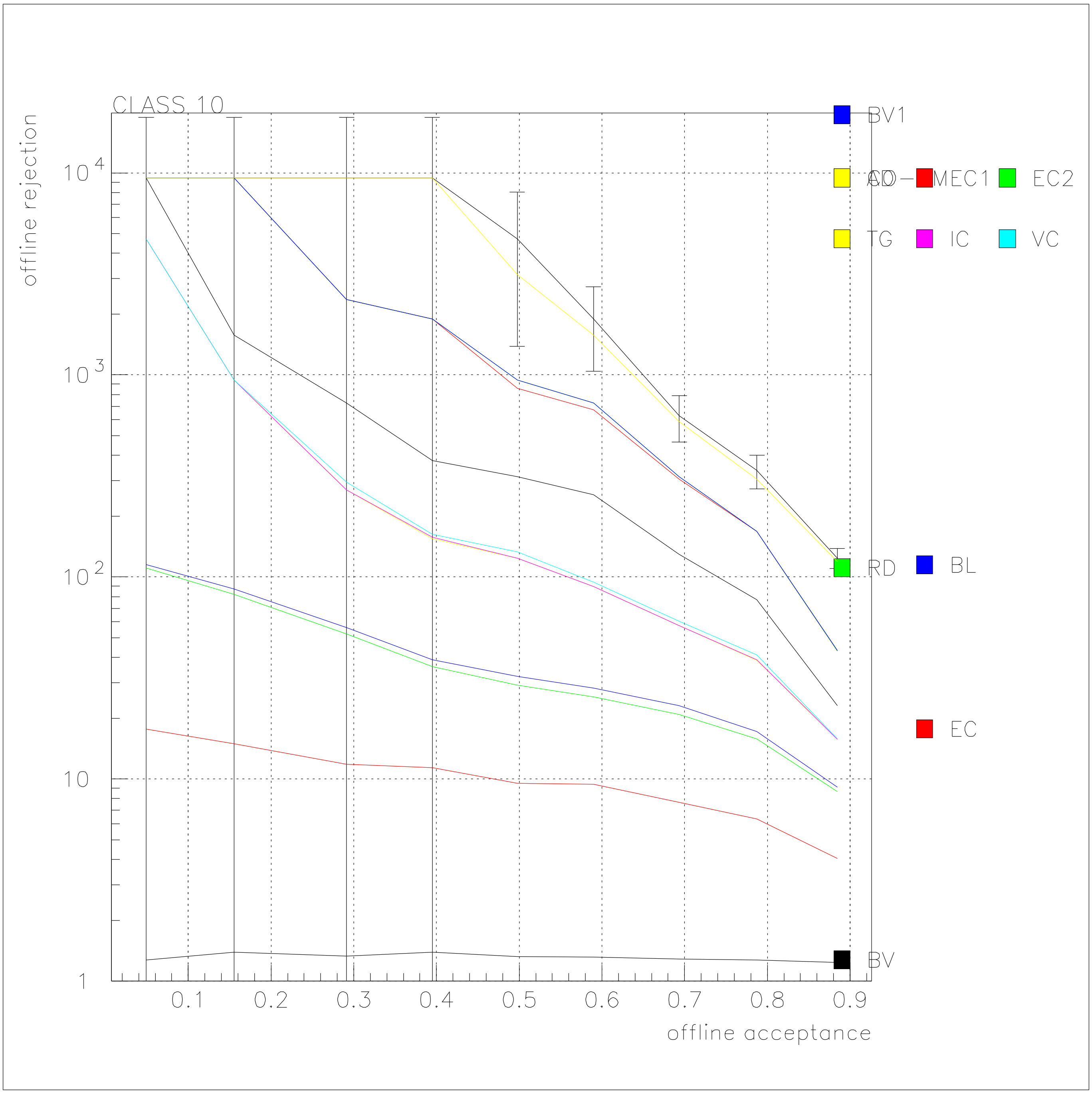

Figure 8: Offline rejection vs acceptance profile for class 10, with each subsystem contribution.

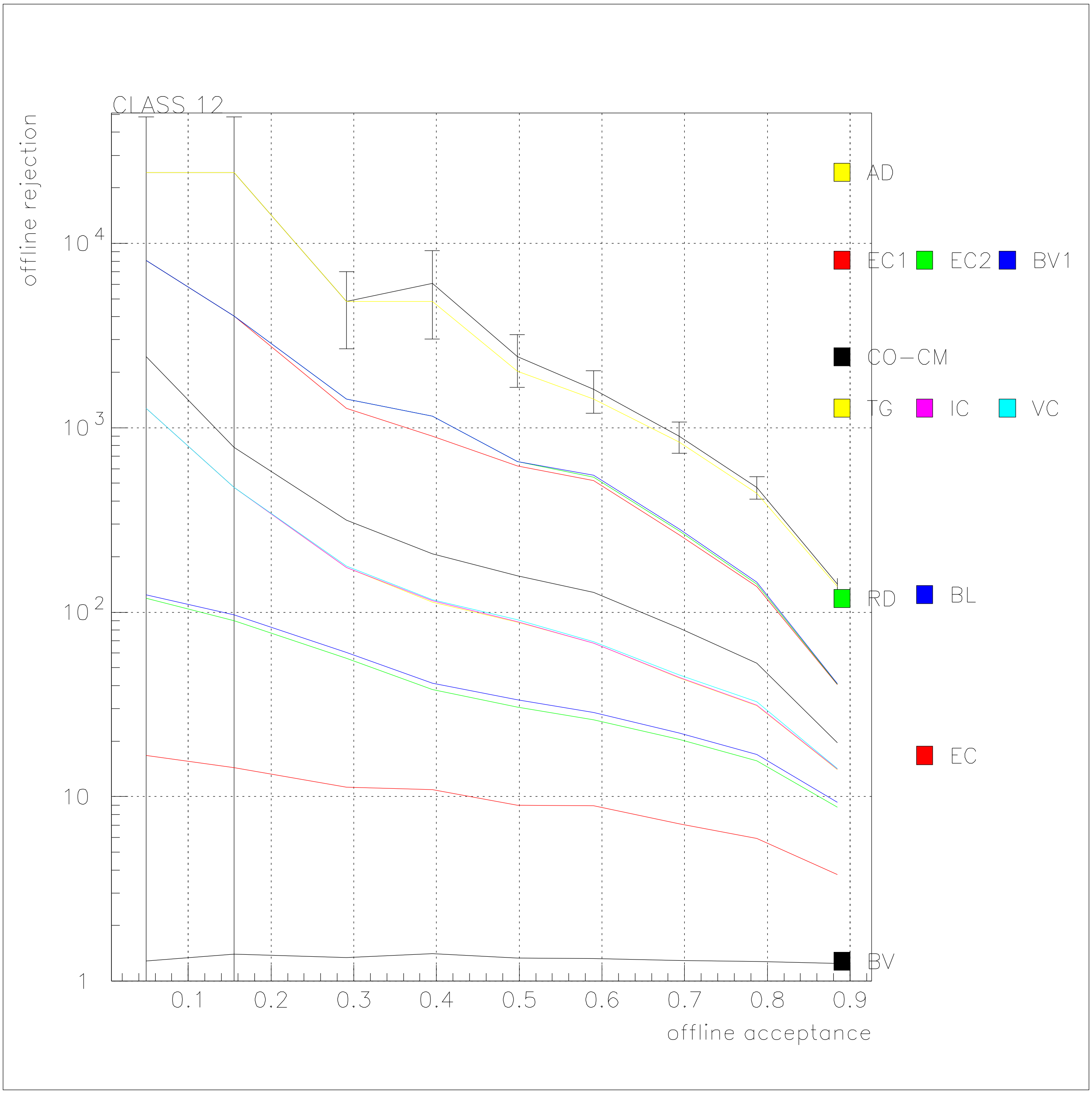

Figure 9: Offline rejection vs acceptance profile for class 12, with each subsystem contribution.

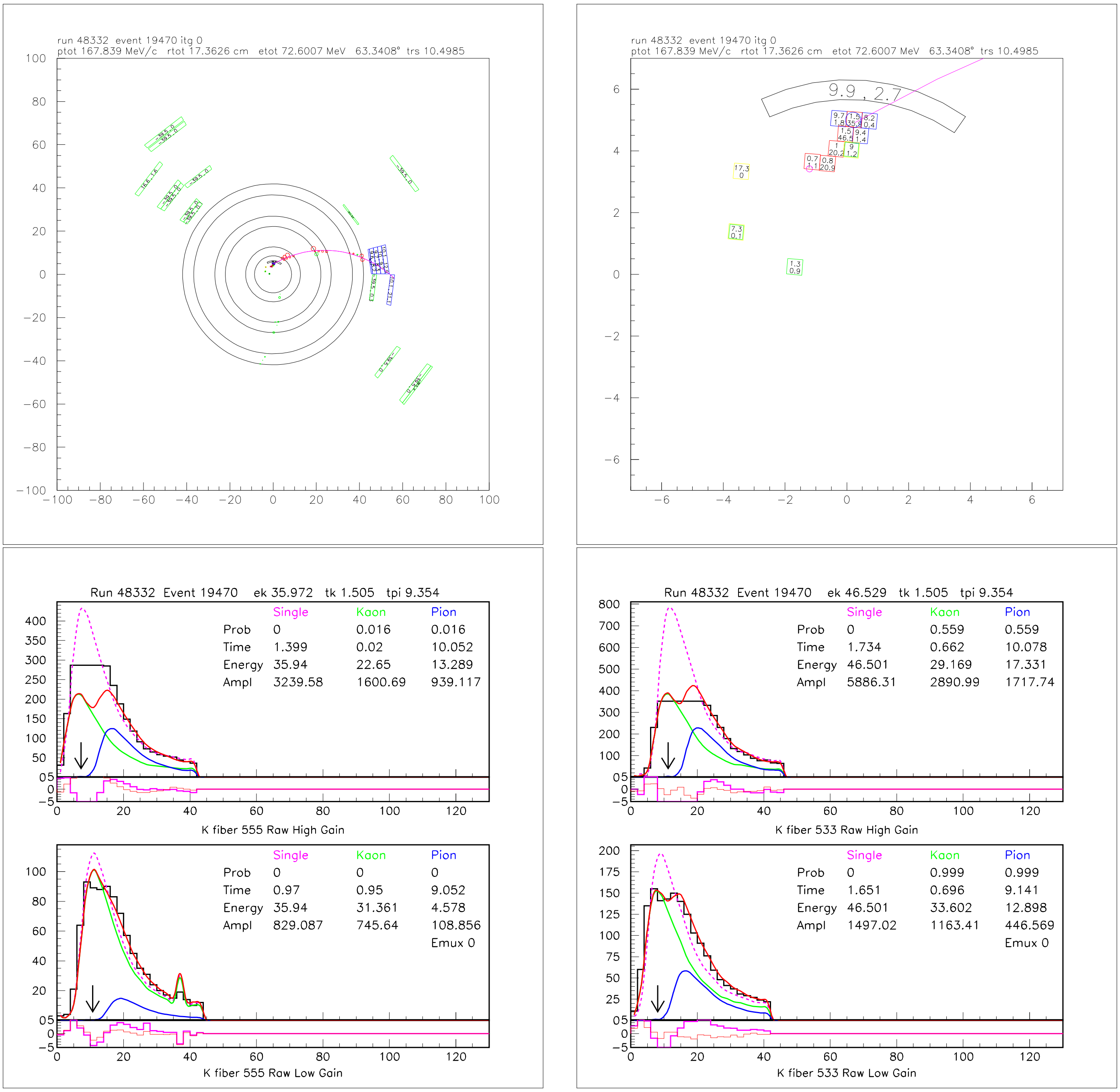

Figure 10: The K_{e4} event: whole detector xy view, TG zoom, CCD pulses in the vertex fiber and the K fiber next to it. The π^- and e^+ dump their energy in the two K fibers and the π and γ fibers surrounding them, which do not seem to belong to the π^+ path. Thus the event fails CCDPUL, CHI567 and other cuts.

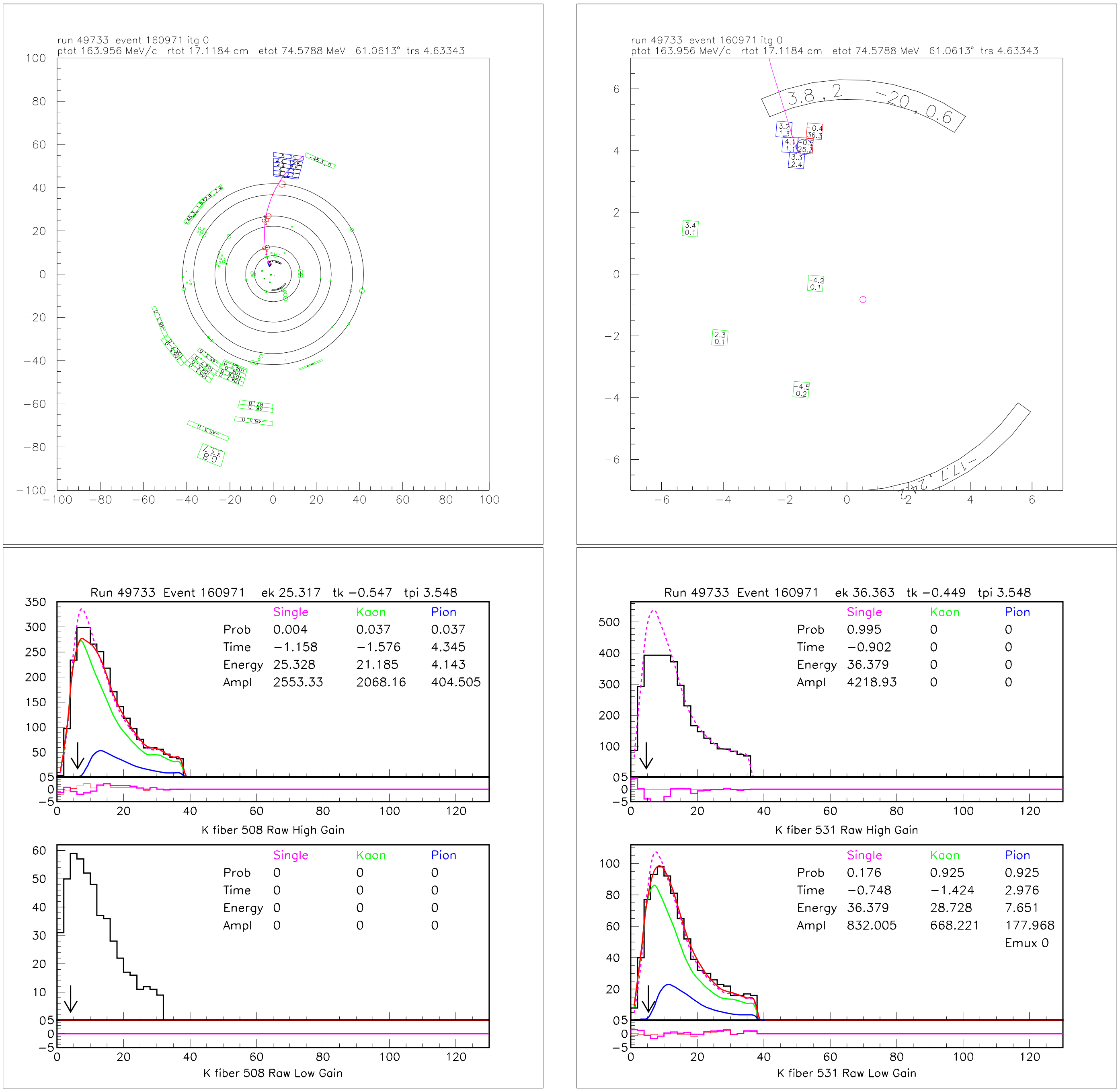

Figure 11: The possible K_{e4} event: whole detector xy view, TG zoom, CCD pulses in the vertex fiber and the K fiber next to it. If it is indeed K_{e4}, the π^- and e^+ dump their energy in the K fibers and the 2.4 MeV π fiber, which does not seem to belong to the π^+ path. Another possibility is that the decay vertex has been misassigned, since there is no reliable B4 information, and was chosen to be on the wrong side of the kaon cluster. There is even some B4 activity near the so called "vertex" fiber. If this is the case, a $K_{\pi 2}$ π^+ could start under the kaon fibers causing the second pulses, and then scatter in the 2.4 MeV π fiber. In any case, the event fails CCDPUL, CHI567 and other cuts.

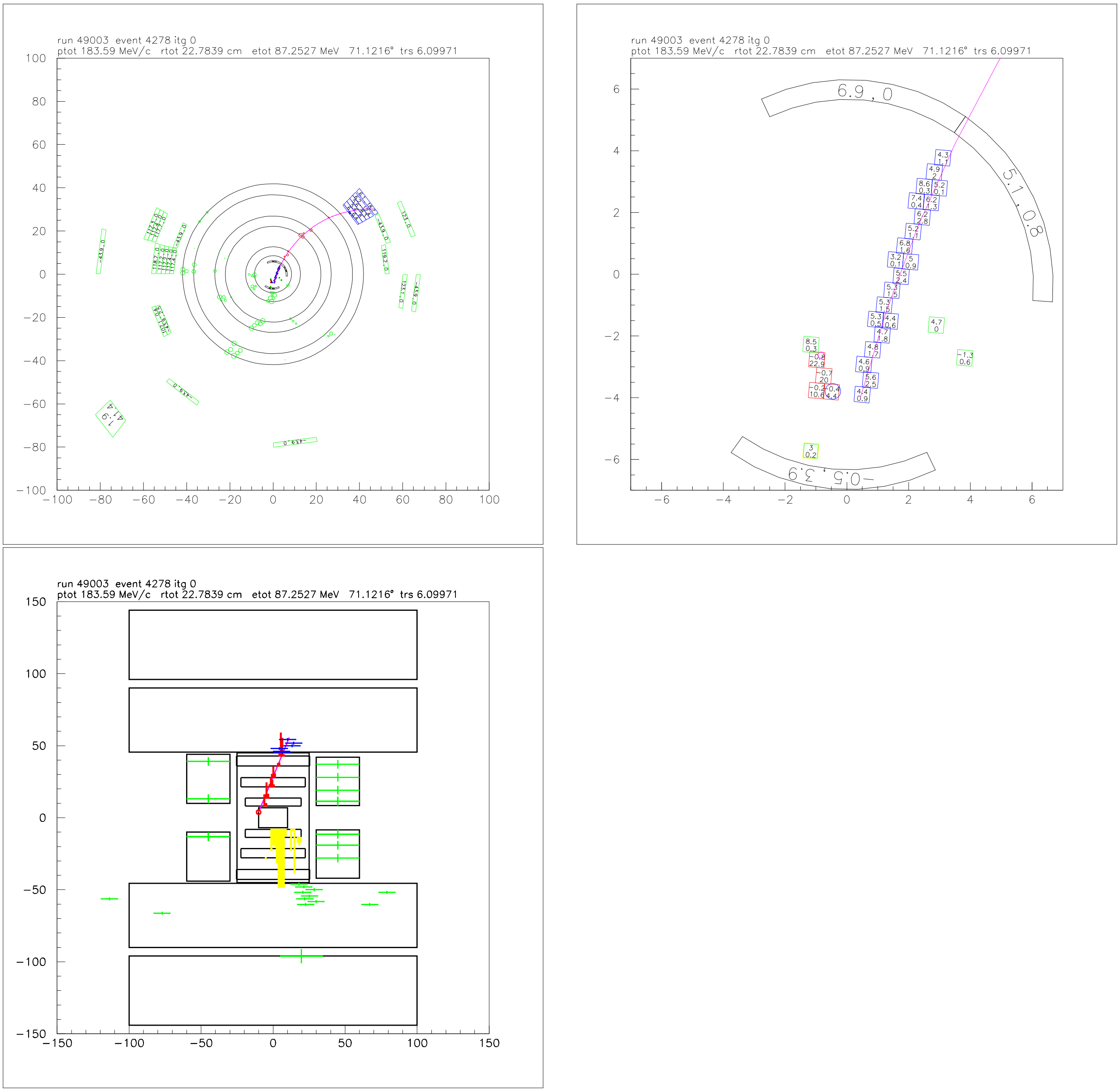

Figure 12: The 2-beam event: whole detector xy view, TG zoom and z view. All the K fibers have no activity at trs. The first kaon decay products are lost, and the pion enters from the face of the TG at trs causing the event to fail a number of cuts (VERRNG, B4EKZ, TARGF, TGZFOOL, KIC...)

CUT	No box	PNN2BOX		KP2BOX
		sequential	last	
	12856573			
BAD_RUN,KERROR	12525587			
SKIM5,RECON	8156752			
PSCUT06	2730052			
DELCO3	2713349			
TDCUT02	699267			
KINCUT06	409159			
$\overline{PVCUT}$		38078		330814
B4EKZ(IC)		27242 (1.39777)	3687 (1.17346)	301449
TGZFOOL		26853 (1.01449)	3755 (1.01844)	296595
EPITG		16889 (1.58997)	3759 (1.01953)	260545
EPIMAXK		16889 (1)	3687 (1)	260545
TARGF		14397 (1.17309)	3789 (1.02766)	251761
DTGTTP		14397 (1)	3687 (1)	251753
RTDIF		14287 (1.0077)	3713 (1.00705)	249613
DRP		14091 (1.01391)	3699 (1.00325)	248758
TGKTIM		13852 (1.01725)	3713 (1.00705)	246332
EIC		13560 (1.02153)	3763 (1.02061)	242238
TIC		13560 (1)	3687 (1)	242237
TGEDGE		13343 (1.01626)	3725 (1.01031)	239972
TGDEDX		12547 (1.06344)	3746 (1.016)	238494
TGENR		12277 (1.02199)	3751 (1.01736)	232184
PIGAP		12091 (1.01538)	3701 (1.0038)	230556
TGB4		10860 (1.11335)	3896 (1.05669)	216849
KIC		10854 (1.00055)	3690 (1.00081)	216747
PHIVTX		8128 (1.33538)	4097 (1.1112)	209500
OPSVETO		7100 (1.14479)	4204 (1.14022)	200239
TGLIKE		6691 (1.06113)	3821 (1.03634)	193841
TIMKF		5448 (1.22816)	4623 (1.25386)	172474
NPITG		5448 (1)	3687 (1)	172474
ALLKFIT		5202 (1.04729)	3905 (1.05913)	166539
TPICS		5198 (1.00077)	3692 (1.00136)	166511
EPIONK		4906 (1.05952)	3900 (1.05777)	158435
CHI567		4037 (1.21526)	4130 (1.12015)	135866
VERRNG		3377 (1.19544)	4452 (1.20749)	127354
CHI5MAX		3150 (1.07206)	3958 (1.0735)	118701
ANGLI		3142 (1.00255)	3697 (1.00271)	118633
CCDBADFIT		2860 (1.0986)	0 (0)	107477
CCDPUL		498 (5.74297)	0 (0)	56161

Table 3: The normalization branch for the $K_{\pi 2}$ TG scatter background: events after setup cuts and TGCUTS and their rejection (in brackets), for every TGCUT applied sequentially or last, for $\pi\nu\overline{\nu}(2)$ and $K_{\pi 2}$ boxes.

Description	Events (all classes)	Events (class 12)
$K_{\pi 2}$ TG scatter	9	8
K_{e4}	1	1
Possible K_{e4}	1	1
2-beam	2	1
"TARGF" event	1	0
TOTAL	14	11

Table 4: Categorization of the events surviving after all cuts in the rejection branch in all classes and class 12 separately. The "TARGF" event is an unidentified single-cut-failure (more information in the single-cut-failure study zoo in [6]).

CUT	Rejection		Normalization	
	PBOX from KP2BOX		$\overline{RSDEDX}$ or $\overline{PRRF}$	
	KP2BOX	PNN2 RE BOX	KP2BOX	PNN2BOX
SETUP	86172	681	23249	212
LAYER14	86114	681	23230	212
FIDUCIAL	79180	615	20880	197
UTCQUAL	76665	602	20030	177
RNGMOM	76030	602	19834	154
RSDEDX	66354	106	NA	NA
PRRF	56196	78	NA	NA
PVCUT	35	0	9	0

Table 5: Background study for $K_{\pi 2}$ RS scatters. PBOX is the momentum cut and RE BOX the range and energy cut. "NA" means that the cut is not applied, because the RSCT cuts have been reversed in the normalization branch.